Spectroscopy of ^{204,206,208}Rn and the systematic behavior of $Z = 86$ isotopes

D. Horn,* C. Baktash, and C. J. Lister[†]

Brookhaven National Laboratory, Upton, New York 11973

A spectroscopic investigation of the radon isotopes ^{204,206,208}Rn was performed by means of the reactions ^{192,194,196}Pt(^{16}O,$4n$)^{204,206,208}Rn and ^{197}Au(^{14}N,$5n$)^{206}Rn with ^{16}O energies between 85 and 110 MeV and ^{14}N energies between 80 and 94 MeV. γ-γ coincidences, pulsed beam yield functions, angular distributions, and pulsed beam isomeric decay rates were measured. The yrast and near-yrast level structure was established to $J \sim 15\hbar$, and in each of the three nuclei two isomers above the known $J^{\pi}=8^{+}$ state were observed. The systematic trends for the $Z = 86$ isotopes are compared with the behavior expected in a single particle model, and increased collectivity is found with decreasing neutron number. Analogies are made with the $N = 86$ system.

I. INTRODUCTION

Interest has in recent years been focused near the $N = 82$ and $Z = 82$ shell closures, where states of large angular momentum, formed by the alignment of valence nucleons in high-j orbitals, have been observed. In particular, the $N=86$ isotones[1] and the $Z = 86$ isotopes,[2-5] with four valence nucleons in the $f_{7/2}$, $h_{9/2}$, and $i_{13/2}$ orbitals, have been fertile ground in the spectroscopy of discrete γ rays from high spin states. Information concerning the collectivity and deformation in such particle-aligned states would be valuable, and it is especially in this respect that the systematic behavior of the (even) $Z = 86$ isotopes is significant.

The isotopes $^{210}_{86}$Rn$_{124}$ (Ref. 4), and $^{212}_{86}$Rn$_{126}$ (Refs. 2 and 3) have already been investigated to high spins, and work is in progress on the nucleus $^{214}_{86}$Rn$_{128}$ (Ref. 5), which has two valence neutrons in addition to its four valence protons.

The present study is a detailed spectroscopic investigation of the nuclei ^{204,206,208}Rn to excitation energies of about 4 MeV and spins of about $15\hbar$. Two isomers have been observed in each nucleus above the previously known $J^{\pi}=8^{+}$ levels. Earlier work by Inamura et al.[6] (^{206}Rn, in-beam gamma

ray studies), Ritchie[7] (^{206,208}Rn, isotope-separated gamma ray studies), and Backe et al.[8] (^{204,206,208}Rn gamma ray and conversion electron measurements) had established the structure of these nuclei up to excitation energies of about 2 MeV and spins of about $8\hbar$. A recent report by Backe et al.[9] extends their work in ^{208}Rn to high-lying levels.

Experimental techniques and data analysis for the present work are described in Sec. II; the resulting level schemes for ^{204}Rn, ^{206}Rn, and ^{208}Rn are presented in Secs. III, IV, and V, respectively. Section VI discusses these results in light of the $Z = 86$ systematics, and the work is summarized in Sec. VII.

II. EXPERIMENTS AND DATA ANALYSIS

The nuclei were produced by the ^{192,194,196}Pt(^{16}O,$4n$)^{204,206,208}Rn and the ^{197}Au(^{14}N,$5n$)^{206}Rn reactions. The Brookhaven National Laboratory Tandem Van de Graaff facility provided beams of ^{16}O from $85-110$ MeV and ^{14}N from $80-94$ MeV. Targets were backed with thick ($8-10$ mg/cm^2) layers of isotopically separated ^{208}Pb to stop the recoils and improve re-

tention of spin alignment. The platinum targets were 3—4 mg/cm^2 in thickness. The ^{192}Pt target was enriched to 57%, the ^{194}Pt target to 97%, and the ^{196}Pt target to 98%. The ^{197}Au target was 6 mg/cm^2 in thickness.

Gamma ray yields as a function of bombarding energy were measured in order to assign transitions to given isotopes, to determine the most favorable bombarding energy for populating the higher-lying states, and to aid in relative ordering of the transitions. In the case of ^{206}Rn, an excitation function with a pulsed ^{14}N beam made possible the ordering of the delayed cascade deexciting the $J^\pi = 6^+$ state, a point of disagreement between earlier investigators.[6-8] The amounts of delayed feeding compared to prompt feeding at each level were taken to indicate proximity to the isomer.

The gamma-gamma coincidence events were recorded on tape and analyzed in terms of the time relationship between the coincident gamma rays. Figure 1 shows γ rays in prompt and delayed coincidence with the 542.9- and 588.5-keV transitions in ^{204}Rn. The measurement was made with a 96 MeV ^{16}O beam. Panel (a) shows Ge(Li) pulses arriving ~ 15 nsec or more before the gates; events occurring in prompt coincidence, that is, within ~ 15 nsec of the 542.9- or 588.5-keV gating transitions, are displayed in panel (b). Note the presence of "prompt" gamma rays in the "before" spectrum of panel (a). This is due primarily to nonuniformities in rise times for the various pulses, and to the narrowness of the time interval required. Figure 1, to-

gether with related coincidence spectra, indicates two parallel decay paths of comparable intensity feeding the lowest two transitions. This phenomenon is not seen in the other radon isotopes studied.

A similar set of spectra for ^{206}Rn, measured using a ^{16}O beam of 92.5 MeV, is shown in Fig. 2. The gating transitions here, 559.1, 575.4, and 628.8 keV, deexcite the three lowest-lying levels in ^{206}Rn. Panel (a) represents those γ-rays preceding the gating transitions by ~ 30 nsec or more, and in panel (b) the four strongest lines are from the cascade deexciting the previously known $J^\pi = 8^+$ state. Several strong lines in the before spectrum are also weakly visible in panel (b): the 205.7-, 346.0-, 551.2-, and 610.3-keV transitions. This indicates their separation from the lowest-lying cascade is a few tens of nonoseconds, while the remaining precursors feed a longer isomer.

In Fig. 3, a delayed coincidence spectrum is displayed for the nucleus ^{208}Rn. The measurement was made with a 90 MeV ^{16}O beam, pulsed at 1 μsec intervals. The gating transition is 789.6 keV, which, we find, must lie isolated by isomers both above and below since panel (a) shows precursors in abundance, panel (b) shows no γ-ray peaks in prompt (within ~ 30 nsec) coincidence, and panel (c) shows the three lowest-lying transitions detected later in time.

Decay rates were measured using pulsed ^{16}O beams, typically 8 nsec FWHM, at the same beam energies used in the coincidence runs. In addition to their obvious use in obtaining transition rates, the
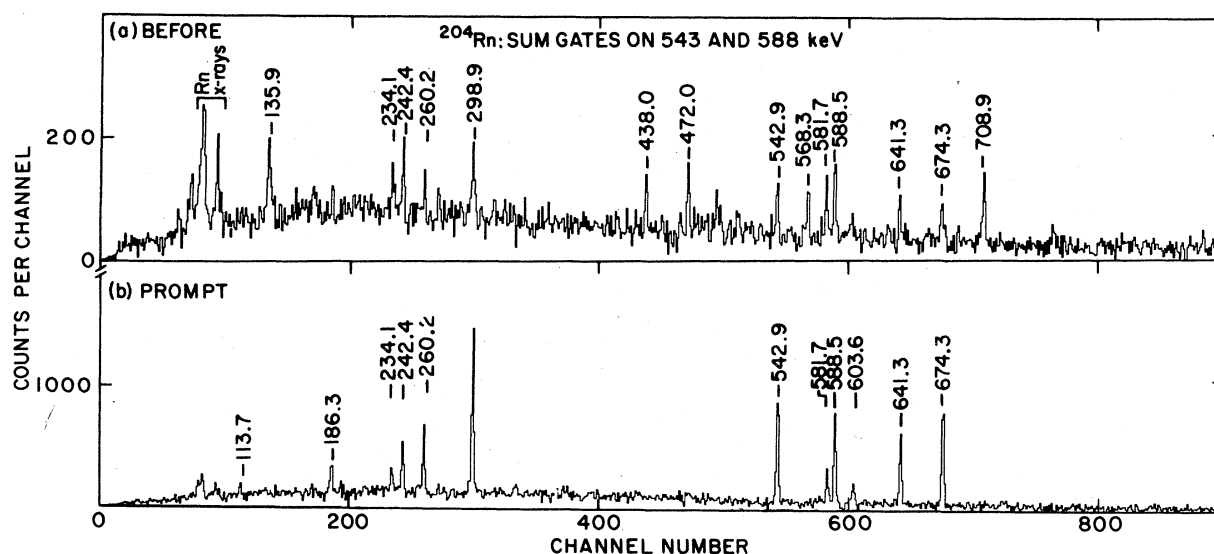

FIG. 1. ^{204}Rn γ-γ delayed coincidence spectra, gated by a sum of the 543- and 588-keV transitions. Energies labeled are in keV. See text for the discussion of individual panels.
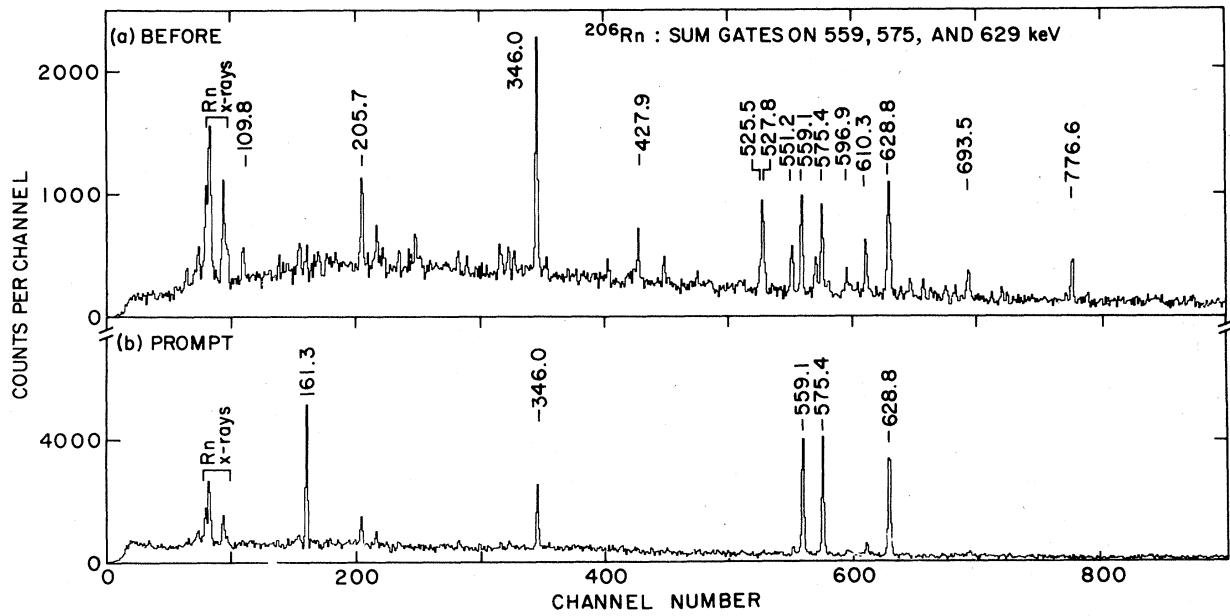
FIG. 2. ^{206}Rn γ-γ delayed coincidence spectra, gated by a sum of the 559-, 575-, and 629-keV transitions. Energies labeled are in keV. See text for the discussion of individual panels.
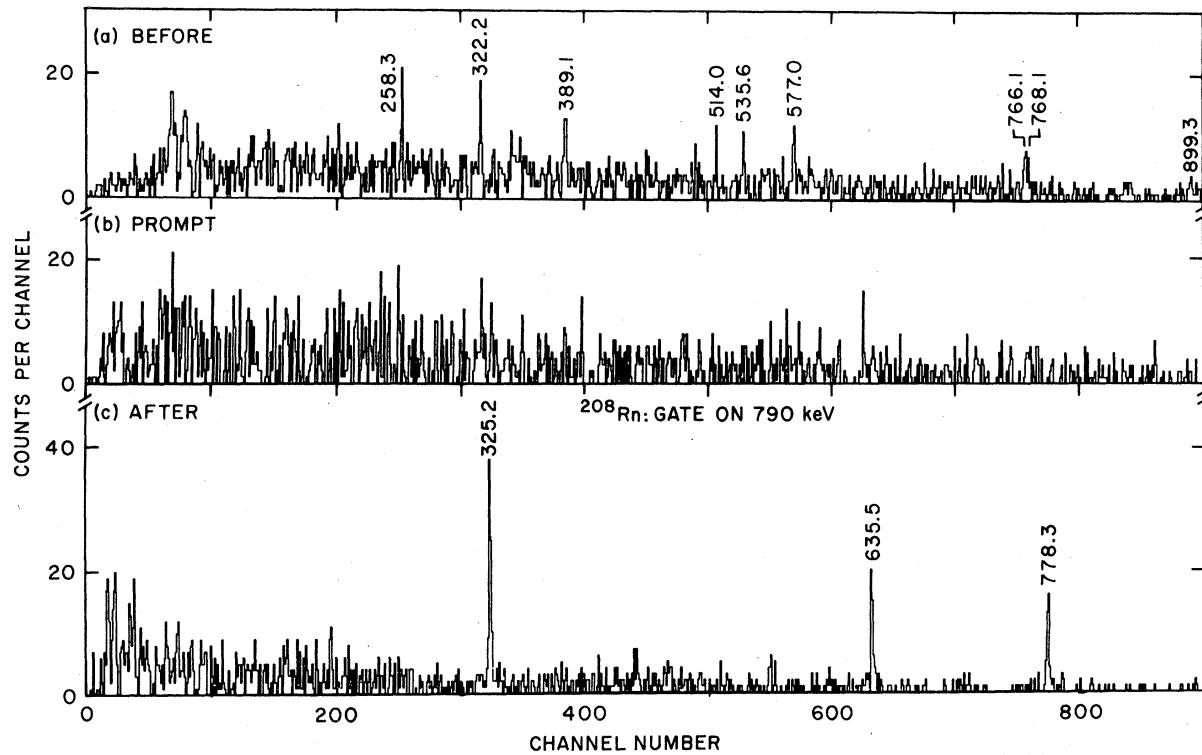
FIG. 3. ^{208}Rn γ-γ delayed coincidence spectra gated by the 790-keV transition. Energies labeled are in keV. See text for the discussion of individual panels.

pulsed beam measurements provided further constraints in the assembly of the level schemes. Naturally, the decay curve for a transition directly deexciting an isomer should show no prompt peak. If the highest-lying transition observed in an isomeric cascade had a prompt component, then a transition, unobserved due to its low energy or high conversion coefficient, might exist, directly deexciting the isomer. In fact, the amount of prompt feeding displayed by transitions might be used to establish the relative ordering of γ rays in a delayed cascade.

Examination of the decay curves for the 234.1- and 581.7-keV transitions in ^{204}Rn reveals a high lying isomer with a half-life of about 10 nsec [Fig. 4, panel (a)]. This isomer has been observed only weakly, and its location ($E_{ex} \simeq 4$ MeV) is uncertain. The 242.4 keV transition [panel (b)] directly deexcites a longer and more distinctly observed isomer of half-life $T_{1/2} = 33 \pm 3$ nsec, and the 542.9 keV ground state transition [panel (c)] shows the same lifetime with a substantial peak from prompt sidefeeding. The nucleus ^{206}Rn has an isomer at 4130 keV with $T_{1/2} = 11 \pm 2$ nsec, as manifested by the 776.6 keV γ ray in Fig 5, panel (a). Panel (b) shows the decay of the $T_{1/2} = 65 \pm 5$ nsec isomer at $E_{ex} = 2476$ keV through a 551.2 keV transition. The lack of a prompt component in the time spectrum suggests that this transition directly deexcites the isomer. In panel (c) the ground state transition (575.4 keV) is shown to contain the same 65 nsec half-life plus an additional $T_{1/2} = 19 \pm 3$ nsec

component from the $E_{ex} = 1925$ keV isomer, obtainable when the decay curve is fitted using a two-level decay program. A search for longer lifetimes ($T_{1/2} < 0.05$ sec) using mechanical and electrostatic beam choppers was made for this nucleus. No such long lived isomers were observed. Figure 6 shows decay curves for ^{208}Rn, including a high-lying ($E_{ex} \simeq 4$ MeV) isomer with $T_{1/2} = 20 \pm 2$ nsec observed through the 322.2-, 577.0-, and 768.1-keV transitions in panel (a) and the $E_{ex} = 2617$ keV isomer with a half-life of $T_{1/2} = 17 \pm 3$ nsec, obtained by fitting the 789.6-keV decay curve with a two-level program, fixing the upper isomer at $T_{1/2} = 20$ nsec. In panel (c) the decay curve for the sum of the 325.7- and 778.3-keV transitions is shown. The $T_{1/2} = 473 \pm 11$ nsec half-life for this $E_{ex} = 1827$ keV isomer is obtained from a two-isomer fit which also gives a composite 22 nsec feeding time.

Angular distribution measurements for ^{204}Rn and ^{208}Rn were performed at ^{16}O bombarding energies of 95 and 92 MeV, respectively. ^{206}Rn was studied using the ^{197}Au(^{14}N,5n) reaction with a ^{14}N beam of 88 MeV, and the ^{194}Pt(^{16}O,4n) reaction at 95 MeV, using the contaminant reaction from the "^{192}Pt" target, which was approximately 40% ^{194}Pt. This provided confirmation for the observed values and information on spectrum peaks obscured in one reaction or the other. Tables I—III present angular distribution and intensity information for the more prominent transitions in ^{204}Rn, ^{206}Rn, and ^{208}Rn, respectively. Uncertainties in the
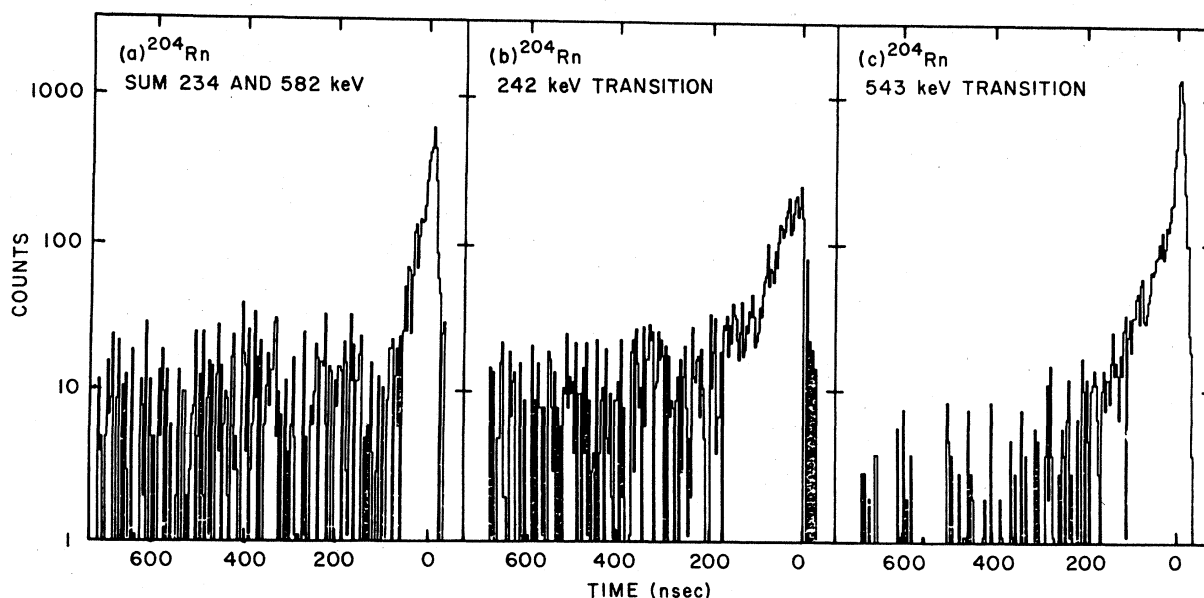

FIG. 4. Isomer decay curves for ^{204}Rn. See text for fitted half-life values.
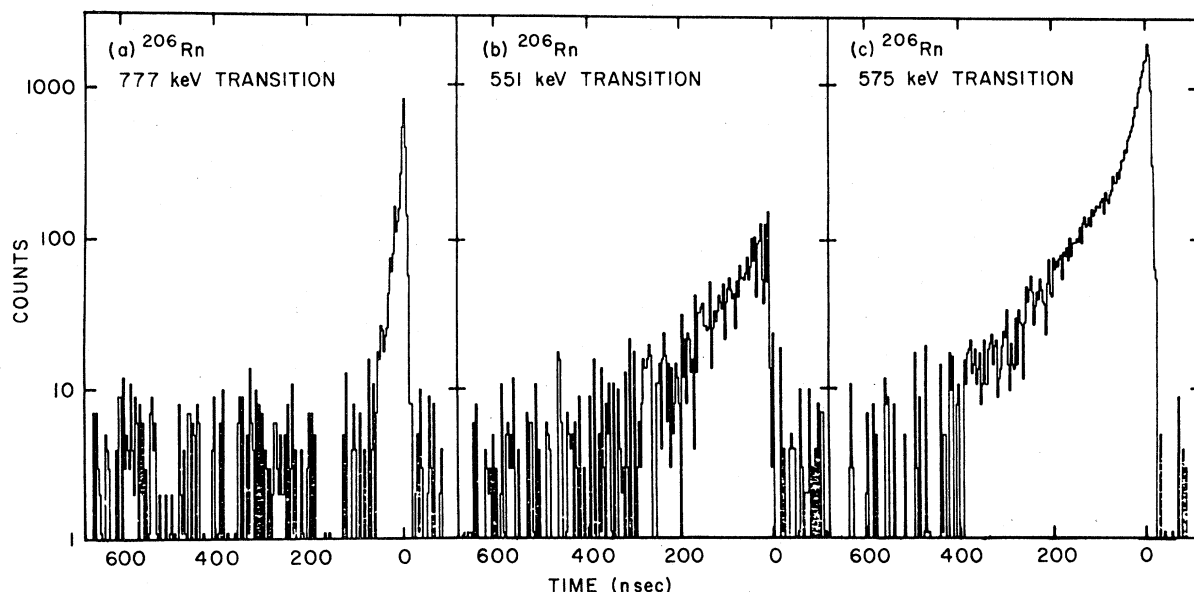
FIG. 5. Isomer decay curves for ^{206}Rn. See text for fitted half-life values.

transition energies range from 0.1 to 0.3 keV. Gamma-ray intensities are shown corrected for conversion[10] and expressed as a percentage of the ground state transition intensity. Where electric as well as magnetic character is possible, both intensities are shown. Intensities are taken from the A_0 coefficient of the Legendre polynomial fitted to the angular distribution unless the line is weak or contaminated by other gamma rays, in which case the

coincidence intensity is used. Owing to the abundance of isomers in these nuclei, spin alignment is generally severely attenuated. In particular, the $a_4 \equiv A_4/A_0$ terms of the fitted Legendre polynomials are frequently small or uncertain. Therefore, when consistent with zero (one standard deviation or less) those values have been omitted from the tables. It should be noted that throughout these isotopes unusually high negative $a_2 \equiv A_2/A_0$
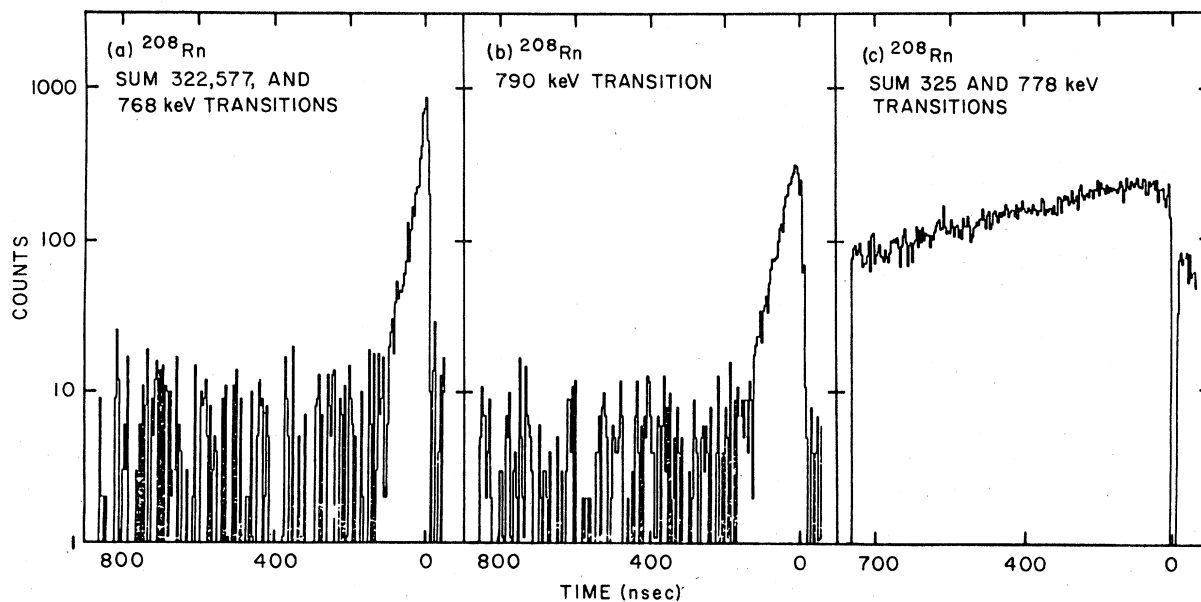

FIG. 6. Isomer decay curves for ^{208}Rn. See text for fitted half-life values.

TABLE I. Gamma rays in ^{204}Rn from the reaction of 95 MeV ^{16}O with ^{192}Pt: conversion-corrected intensities and Legendre polynomial angular distribution coefficients. Uncertainties are in parentheses. Only the more intense lines are listed.

E_γ	I_γ (%)	a_2	a_4
113.7	20[a]	−0.18(10)	
135.9	29	−0.26(14)	
186.3	19	−0.31(15)	
234.1	19/40[b]	0.00(5)	
242.4	24/50[b]	−0.22(11)	
260.2	30	0.07(5)	
298.9	51[a]	0.16(3)	
542.9	100	0.15(1)	
581.7	20[a]	0.11(7)	
588.5	95[a]	0.10(1)	
641.3	37	0.11(3)	
674.8	57	0.04(4)	
708.6	12	0.25(5)	

[a]Weak or contaminated line. Intensity estimated from coincidence yields.
[b]Conversion corrected yield for an $E1/M1$ character where either is possible.

values were observed, raising the question of a possible systematic error in our measurement.

III. ^{204}Rn LEVELS

The ^{204}Rn level scheme is shown in Fig. 7. Intensities are indicated by the width of the transition arrows and correspond to the values in the tables. The cascade deexciting the $J^\pi = 8^+$ level at

excitation energy E_{ex} = 2105 keV is in agreement with the work of Backe et al.[8] However, a parallel branch deexciting a lower-lying $J^\pi = 8^+$ state (E_{ex} = 2033 keV) is also present. Both branches are fed from a $J^\pi = 9^-$ state at 2219 keV excitation. The parity is determined by the assignment of an $E1$ character to the 113.7 keV dipole transition, since

TABLE II. Gamma rays in ^{206}Rn: conversion corrected intensities and Legendre polynomial coefficients. Uncertainties are in parentheses. Only the more intense lines are listed.

E_γ	88 MeV ^{14}N + ^{197}Au			95 MeV ^{16}O + ^{194}Pt		
	I_γ (%)	a_2	a_4	I_γ (%)	a_2	a_4
109.8	4	−0.20(13)		13	−0.11(37)	
161.3	120	0.11(7)		90[a]	0.06(2)	−0.48(32)
205.7	32	−0.06(5)	0.17(8)	31	−0.38(11)	0.40(16)
248.9	5/10[b]	−0.26(6)		4/8[b]	−0.52(9)	
346.0	46	−0.08(2)		55	0.01(3)	
427.9	6	0.32(7)		32	−0.02(3)	−0.40(40)
525.5	4/5[b]	−0.56(40)		6/7[b]	−0.13(30)	
527.8	16/18[b]	−0.55(4)	0.64(61)	18/20[b]	−0.50(6)	
551.2	16	0.00(3)		30	0.03(6)	
559.1	98	0.13(1)		104	0.16(2)	0.31(22)
575.4	100	0.13(2)		100	0.15(1)	
596.9	9	0.04(3)	0.25(6)	20	0.16(5)	0.16(7)
610.3	16	0.34(10)		26	0.21(10)	
628.8	93	0.11(3)		97	0.12(1)	−0.48(16)
776.6	13	0.22(3)	−0.45(46)	15	0.18(18)	0.29(28)

[a]Weak or contaminated line. Intensity estimated from coincidence yields.
[b]Conversion corrected yield for an $E1/M1$ character where either is possible.

TABLE III. Intense gamma rays in ^{208}Rn from the reaction of 92 MeV ^{16}O with ^{196}Pt: conversion corrected intensities and Legendre polynomial angular distribution coefficients. Uncertainties are in parentheses.

E_γ	I_γ (%)	a_2	a_4
156.1	8/35[a]	−0.19(9)	
225.6	5	0.01(12)	
258.3	13/25[a]	−0.43(3)	
322.2	10/15[a]	−0.46(8)	
325.2	93	0.03(3)	
389.1	7/9	−0.30(20)	
411.9	18	0.02(4)	
490.9	14/16[a]	−0.12(4)	
535.6	21	−0.14(7)	
544.8	9	−0.02(10)	
553.0	9	−0.03(8)	
577.0	19/21[a]	−0.53(7)	
635.5	100	0.09(1)	0.08(2)
636.7	46	0.14(6)	
766.1[b]	16	0.31(4)	
768.1	19	0.18(3)	
778.3	89	0.02(2)	
789.6	38	0.09(3)	0.05(4)

[a]Conversion corrected yield for an $E1/M1$ character where either is possible.
[b]Not placed in level scheme.

the conversion coefficient for magnetic character would be $\alpha_{total} = 9.7$, making the total intensity greater than that of the $2^+ \rightarrow 0^+$ transition.

The 9^- level is fed by a 242.4 keV dipole transition for which a magnetic character is suggested, solely on the basis of its lifetime ($T_{1/2} = 33 \pm 3$ nsec). The decay curve of the 242.2-keV gamma ray [see Fig. 4(b)] shows no prompt feeding. As discussed in the previous section, this makes an unobserved, low-energy transition less likely as the cause of the isomerism, and the $J = 10$ state at $E_{ex} = 2461$ keV is thus assigned negative parity. Above the isomer, the strongest gamma rays are the 708.6-135.9 keV cascade, deexciting a $J = 13$ state at $E_x = 3306$ keV. This level is in turn fed by several weak transitions, observable only in coincidence spectra. Spins are suggested purely on the basis of crossovers and consistency arguments.

The 581.7-234.1 keV cascade (relative ordering unknown) feeding the $J^\pi = 9^-$ state shows evidence of a half-life on the order of 10 nsec. The location of this isomer is not established, so the lifetime is enclosed in parentheses. One possibility is the $E_{ex} = 4096$ keV level, which is deexcited by a low energy (112 keV) transition.

IV. ^{206}Rn LEVELS

Figure 8 shows the level scheme obtained for ^{206}Rn. The notations and symbols are as in the previous figure. The indicated intensities are taken from the ^{14}N + ^{197}Au angular distribution measurement. The cascade deexciting the $T_{1/2} = 19 \pm 3$ nsec isomer is in agreement with previous investigators,[6−8] except in ordering, which agrees with that of Ritchie.[7]

The $J^\pi = 8^+$ isomer is fed by a 596.9−610.3 keV cascade of quadrupole transitions and by a 205.7−346.0 keV cascade of dipole transitions, which is crossed over by a 551.2 keV transition from the isomeric ($T_{1/2} = 65 \pm 5$ nsec), $J = 0$, $E_{ex} = 2476$ keV level. Again, the lack of a prompt component in the decay curve of the 551.2 keV line [Fig. 5(b)] suggests that the isomerism is not caused by an unobserved low energy transition, and consequently indicates that the transition is $M2$ in nature. The $J^\pi = 9$ level at $E_{ex} = 2271$ keV can be assigned negative parity since, when viewed in coincidence with feeding γ rays, such as the 527.8 and 776.6 keV lines, the 205.7 and 346.0 keV transitions should have equal total intensities. This is only
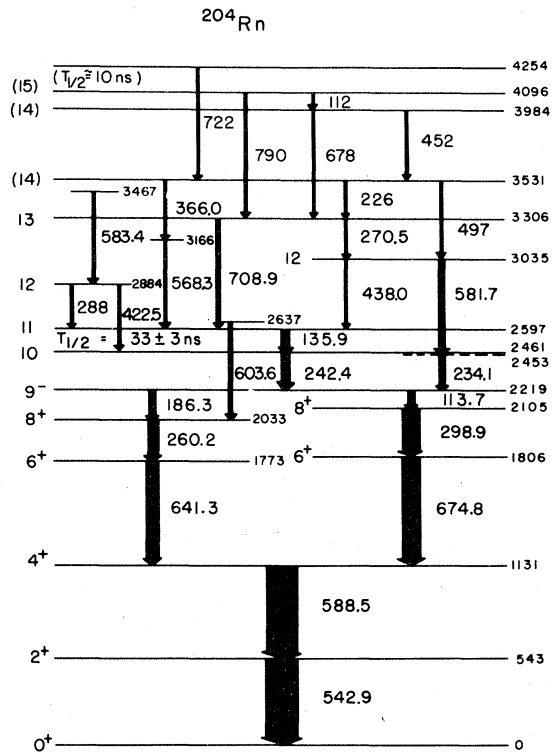
FIG. 7. Level scheme for ^{204}Rn. Energies are in keV. Intensities (corrected for conversion) greater than 0.1 of the $2^+ \rightarrow 0^+$ intensity are indicated by proportionately broadened transition arrows. The measured half-lives of the isomeric states (in nsec) are indicated above the corresponding levels. Uncertain assignments of J or isomer locations are enclosed in parentheses. Tentatively established level positions are indicated by dotted lines.

FIG. 8. Level scheme for ^{206}Rn. Notation as in Fig. 7. Ordering of 110-777- and 249-528-keV sequences is tentative.

achieved when the conversion coefficient for an $M1$ transition, $\alpha \simeq 2$, is applied to the observed 205.7 keV gamma ray intensity.

The $J^\pi = 10^-$ isomer is fed by a 109.8 keV γ ray in coincidence with a pair of dipole transitions which are crossed over by a 776.6 keV quadrupole transition. The relative ordering of these levels is tentative, but there are some indications of low intensity parallel branches feeding from the supposed $E_{ex} = 2834$ keV state into the $E_{ex} = 2586$- and 2476-keV levels. An $E1$ rather than an $M1$ character is suggested for the 109.8-keV γ ray by its observed intensity.

The $J^\pi = 13^{(+)}$ level at 3362 keV excitation is fed by a 768.0-keV γ ray and a 525.5-keV dipole transition. A line of 242-keV is observed in coincidence with the 525.5-keV transition, and the proposed sequence is shown in the figure. Again, relative ordering of the 242- and 525.5-keV γ rays is uncer-
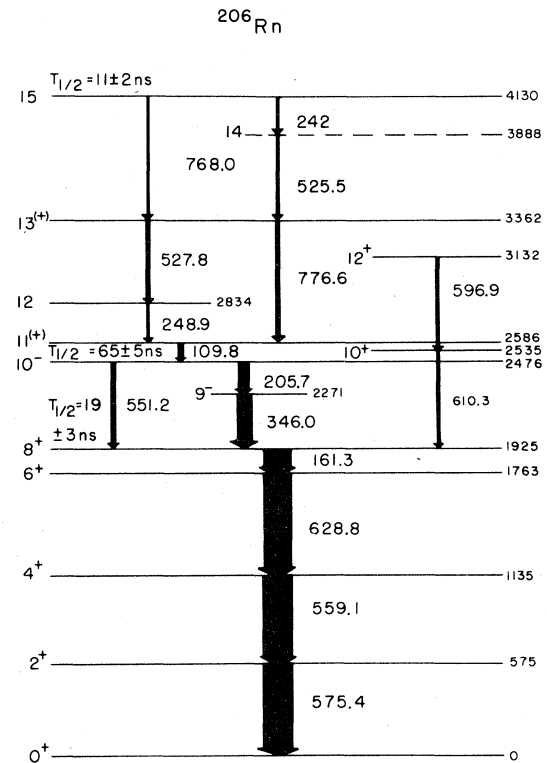
tain. The $T_{1/2} = 11 \pm 2$ nsec isomer apparently is located at $E_{ex} = 4130$ keV, although the possibility that it lies higher cannot be definitely excluded.

V. ^{208}Rn LEVELS

The level scheme proposed for ^{208}Rn is shown in Fig. 9. The notations and symbols are as in the previous two figures. The lower lying levels correspond to those observed by Ritchie[7] and Backe[8] et al., although the $E2$ transition of $86-89$ keV observed by them was not seen in this study due to its high conversion coefficient. The $J^\pi = 8^+$ isomer at $E_{ex} = 1827$ keV was measured to have a half-life of $T_{1/2} = 473 \pm 11$ nsec. A recent report by Backe et al.[9] extends their earlier work in this nucleus to higher excitation. This is in general agreement with the present work up to the $J^\pi = 13^-$ level at 3774 keV in excitation. In their scheme, the $J^\pi = 13^-$ level is fed through a pair of parallel low-energy transitions by a cascade of 89-, 156-, 333-, and 636-keV transition. The present work saw no evidence of coincidence, prompt or delayed, between that

cascade and the 790-keV γ ray, and instead places the 636- and 333-keV lines parallel to the observed transitions between E_{ex} = 1827 and 3774 keV, as indicated in Fig. 9.

While the angular distribution measurements for the 789.6- and 490.9-keV transitions showed $a_2 > 0$ and $a_2 < 0$, respectively, no useful value was obtained for the 298.7 keV transition. The assignment of an $M2$ character to the 789.6-keV transition feeding the $J^\pi = 8^+$ isomer was therefore aided by the conversion electron measurements of Refs. 7 and 9. The E_{ex} = 2318- and 2617-keV levels thus become $J^\pi = 9^-$ and $J^\pi = 10^-$, respectively. The half-life of the $J^\pi = 10^-$ level was measured to be $T_{1/2} = 17 \pm 3$ nsec. Feeding the isomer are several γ-ray cascades. A cascade of three dipole transitions (all $M1$ according to Ref. 9), 322.2, 577.0, and 258.3 keV is bridged in part by an 899.3-keV crossover transition. A cascade of 389.1 keV (dipole) and 768.1 keV ($E2$) transitions also feeds from the $J^\pi = 13^-$ level at $E_{ex} = 3774$ keV into the $J^\pi = 10^-$ isomer.

Above the E_{ex} = 3774 keV level gamma rays of 156.1 and 237.0 keV were observed. All transitions above the $J^\pi = 10^-$ level which were intense enough

for decay rate studies displayed a component of $T_{1/2} = 20 \pm 2$ nsec half-life [see Fig. 6(a)]. The position of the isomer is uncertain, but must lie at or above E_{ex} = 3774 keV. It has been tentatively placed at the uppermost observed level and enclosed in parentheses in the figure.

The cascade including the 332.6- and 636.7-keV gamma rays feeding the $J^\pi = 8^+$ isomer presents a double problem, since both lines are contaminated. The 636.7-keV line slightly overlaps that of the 635.5-keV ground state transition, and the 332.6-keV line coincides with a target transition produced in Coulomb excitation. Nevertheless, due to the long lifetime of the $J^\pi = 8^+$ isomer, one can obtain very good separation of the two $\sim$636-keV components. No coincidence is observed between the 636.7 keV and 789.6 keV γ rays, and a 411.8-keV transition is observed in coincidence with both the 636.7 and 577.0 keV transitions, indicating a possible link to the $J^\pi = 11^-$ level. The 332.6-keV coincidence intensity is substantially less than that of the total contaminated $\sim$333-keV line and is shown, with various connecting transitions, in the level scheme.

VI. DISCUSSION

In the shell model, the high-j orbitals available to the four valence protons of the $Z = 86$ isotopes are $h_{9/2}$, $f_{7/2}$, and $i_{13/2}$. The neutron configurations of the three nuclei studied here are four, six, and eight neutron holes relative to the closed $N = 126$ shell, their applicable high-j orbitals being $2f_{5/2}^{-1}$ and $i_{13/2}^{-1}$. Accordingly, a great many similarities to the corresponding polonium nuclei (two valence protons), may be expected. In Fig. 10, a systematic overview of the even radon isotopes to about 4 MeV in excitation is presented, from ^{204}Rn with eight neutron holes, to the $N = 126$ nucleus, ^{212}Rn. Indeed, many features of the polonium isotopes ^{202,204,206}Po (Ref. 11) recur here: $J^\pi = 8^+$ isomers with lifetimes increasing and excitation energy decreasing as one approaches the closed neutron shell, a set of neutron hole $J^\pi = 9^-$ levels at 2200−2300 keV of excitation energy (also observed in ^{200,202,204}Pb, where they are very long-lived isomers), and shorter isomers at higher energies with spins of about 15$\hbar$.

One difference between the radon and polonium nuclei is the greater involvement of single particle degrees of freedom in the structure of the polonium levels, as indicated by the small ratio of the $8^+ \rightarrow 6^+$ transition energy compared to the $2^+ \rightarrow 0^+$ transition energy. In addition, the $B(E2)$ value for
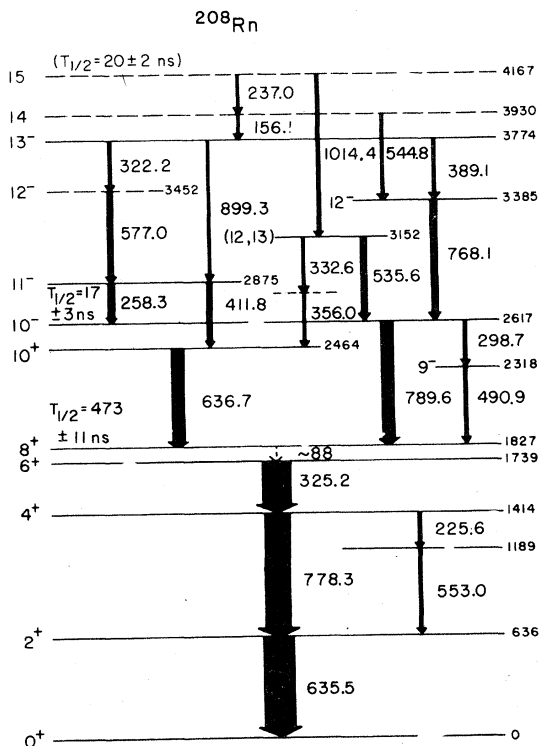

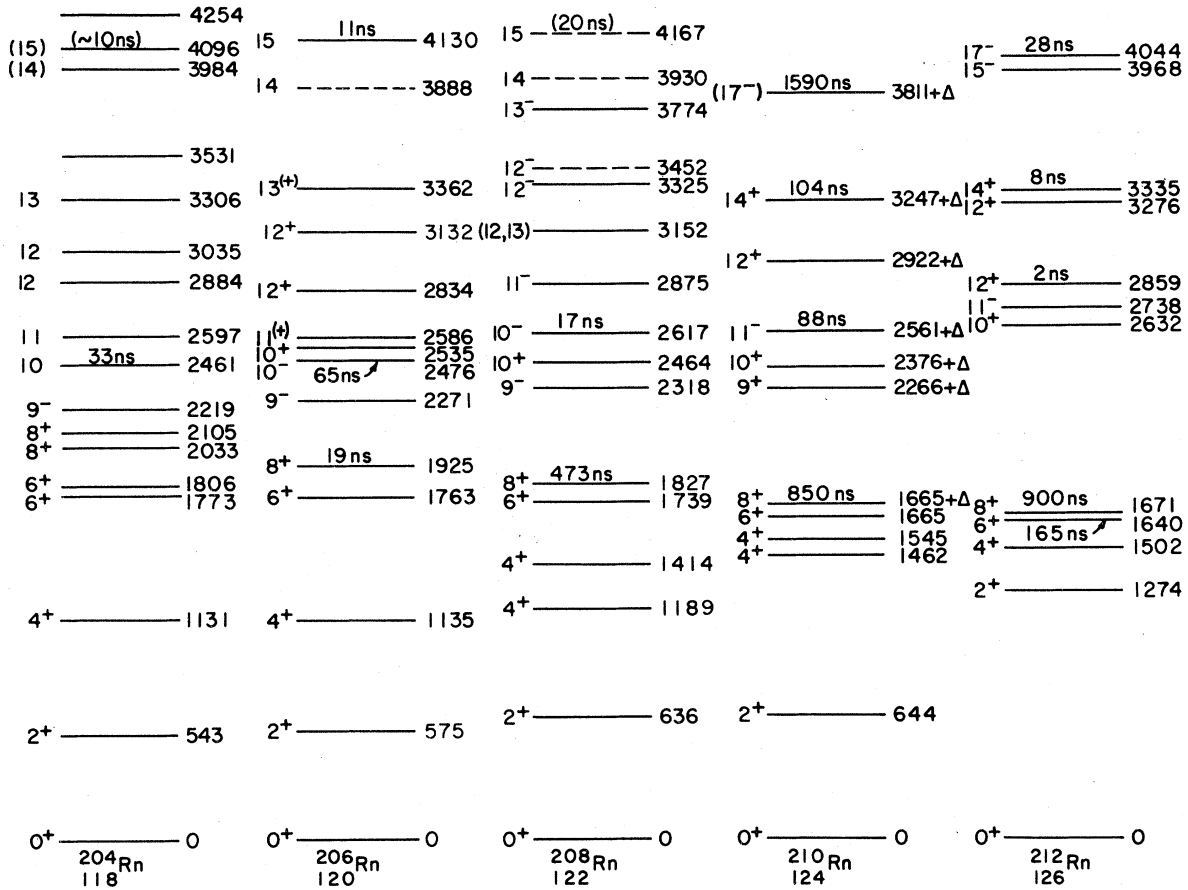FIG. 9. Level scheme for ^{208}Rn. Notation as in Fig. 7.

^{204}Rn (118):
- 4254
- (15) (~10ns) 4096
- (14) 3984
- 3531
- 13 — 3306
- 12 — 3035
- 12 — 2884
- 11 — 2597
- 10 — 33ns 2461
- 9⁻ — 2219
- 8⁺ — 2105
- 8⁺ — 2033
- 6⁺ — 1806
- 6⁺ — 1773
- 4⁺ — 1131
- 2⁺ — 543
- 0⁺ — 0

^{206}Rn (120):
- 15 — 11ns 4130
- 14 — 3888
- 13⁽⁺⁾ — 3362
- 12⁺ — 3132
- 12⁺ — 2834
- 11⁽⁺⁾ — 2586
- 10⁺ — 2535
- 10⁻ 65ns 2476
- 9⁻ — 2271
- 8⁺ — 19ns 1925
- 6⁺ — 1763
- 4⁺ — 1135
- 2⁺ — 575
- 0⁺ — 0

^{208}Rn (122):
- 15 (20ns) 4167
- 14 — 3930
- 13⁻ — 3774
- 12⁻ — 3452
- 12⁻ — 3325
- (12,13) — 3152
- 11⁻ — 2875
- 10⁻ 17ns 2617
- 10⁺ — 2464
- 9⁻ — 2318
- 8⁺ 473ns 1827
- 6⁺ — 1739
- 4⁺ — 1414
- 4⁺ — 1189
- 2⁺ — 636
- 0⁺ — 0

^{210}Rn (124):
- (17⁻) 1590ns 3811+Δ
- 14⁺ 104ns 3247+Δ
- 12⁺ — 2922+Δ
- 11⁻ 88ns 2561+Δ
- 10⁺ — 2376+Δ
- 9⁺ — 2266+Δ
- 8⁺ 850ns 1665+Δ
- 6⁺ — 1665
- 4⁺ — 1545
- 4⁺ — 1462
- 2⁺ — 644
- 0⁺ — 0

^{212}Rn (126):
- 17⁻ 28ns 4044
- 15⁻ — 3968
- 14⁺ 8ns 3335
- 12⁺ — 3276
- 12⁺ 2ns 2859
- 11⁻ — 2738
- 10⁺ — 2632
- 8⁺ 900ns 1671
- 6⁺ 165ns 1640
- 4⁺ — 1502
- 2⁺ — 1274
- 0⁺ — 0

FIG. 10. Systematic behavior of $Z = 86$ isotopes ^{204,206,208,210,212}Rn. Uncertainties indicated by parentheses and dotted levels. Energies are in keV.

the $8^+ \to 6^+$ transitions in the radon isotopes increases rapidly with decreasing neutron number, as discussed in Ref. 8. Using the lower $J^\pi = 8^+$ state observed in ^{204}Rn and lifetimes measured in this work, we obtain $B(E2)$ values of > 100, 127, and 14 e^2fm^4 for ^{204}Rn, and ^{208}Rn, respectively, compared with 11 e^2fm^4 for ^{212}Rn. Undoubtedly, the lower limit for ^{204}Rn could be raised substantially in an experiment sensitive to shorter lifetimes.

These $J^\pi = 8^+$ isomers are predominantly $h_{9/2}$ proton states; however, with decreasing neutron number and increasing collectivity, admixtures of other components must be expected, as indicated by the manifestation of secondary $J^\pi = 8^+$ and 6^+ states in ^{204}Rn. In fact, the work of Ritchie[7] shows a secondary $J^\pi = 6^+$ state in ^{208}Rn and possibly in ^{206}Rn at $E_{ex} = 1825$ and 1819 keV, respectively. The secondary $J^\pi = 6^+$ state in ^{204}Rn is at 1806 keV. Configurations of $f_{7/2}^2$ protons are logical candidates for these states, which vary little in excitation energy, while the energies of $h_{9/2}$ states

vary rapidly with neutron number. Such behavior (constant $f_{7/2}$ level energies, while $h_{9/2}$ level energies vary) has been observed in the region of the $N = 82$ closed shell for valence neutrons.[12] In both regions, going towards more prolate or less oblate ground state configurations raises the energy of the $h_{9/2}$ states relative to $f_{7/2}$ states.

Both in the $N = 82$ region near the closed proton shell and in the $Z = 82$ region near the closed neutron shell, valence nucleons form $(h_{9/2}, i_{13/2})_{11^-}$ states, often with substantial lifetimes.[1,13] It is to be expected that as the energy of the $f_{7/2}$ levels becomes competitive with that of the $h_{9/2}$ levels, $(f_{7/2}, i_{13/2})_{10^-}$ should also become yrast. The series of $J^\pi = 10^-$ levels observed in ^{204,206,208}Rn may be of this nature. The region of these levels is shown enlarged in Fig. 11. If the $J = 10$ isomer in ^{204}Rn were consistent with the adjacent nuclei, then it too would have negative parity. Since no $M2$ transition is observed deexciting the $J = 10$ state in ^{204}Rn, an upper limit of 10% can be put on its observable in-
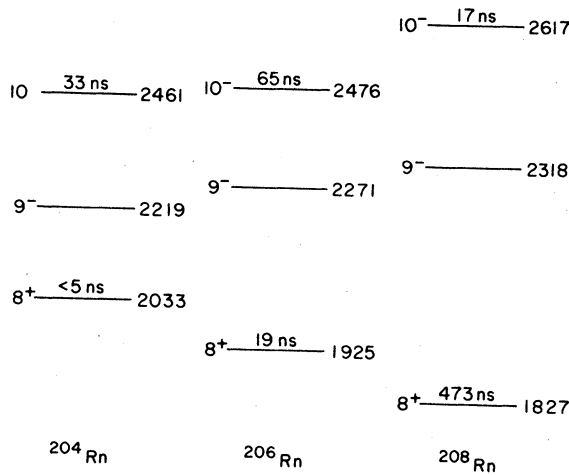
FIG. 11. Enlarged region of $J = 8$ to $J = 10$ systematics for ^{204,206,208}Rn. Energies are in keV.

tensity, yielding an upper limit on its $B(M2)$ value of 17 $(e\hbar/2Mc)^2$fm^2 compared with $B(M2)$ values of 4 and 6 $(e\hbar/2Mc^2)^2$fm^2 for ^{206}Rn and ^{208}Rn, respectively. We observe, then, that the $M1$ transitions are retarded by some five orders of magnitude relative to single particle rates, while the $M2$ transitions, which are probably valence proton transitions, are only slightly retarded. An $M1$ transition from a $(J^\pi = 10^-)$ spin-aligned valence proton configuration to a $(J^\pi = 9^-)$ neutron hole configuration would indeed be expected to be strongly retarded. The 242.4-keV γ-ray deexciting the $J = 10$ level in ^{204}Rn would be an $M1$ transition, with a reduced transition rate of 3.3×10^{-5} $(e\hbar/2Mc)^2$ compared to rates of 1.6×10^{-5} and 1.5×10^{-5} $(e\hbar/2Mc)^2$ in ^{206}Rn and ^{208}Rn, respectively, which go from a spin-aligned valence proton configuration to the neutron hole configuration of the $J^\pi = 9^-$ states.

Levels above the $J = 10$ states (Fig. 10) are somewhat difficult to interpret. The series of isomers at $E_{ex} \cong 4$ MeV and $J \cong 15$ are certainly suggestive of the behavior observed for the corresponding polonium nuclei, but until the positions of the isomers and the spins of the levels are more definitely determined, further specification is of limited value.

It is apparent that the yrast level patterns of the $N = 126$ closed shell isotones[13] with their

$(h_{9/2}{}^3, i_{13/2})$ levels of $J^\pi = 11^-$ and 17^- are destroyed by the removal of core neutrons. Apparently the higher energy cost of the $h_{9/2}$ orbitals raises the yrast line to an energy where both valence proton $f_{7/2}$ and neutron hole configurations can compete successfully. Such systematic raising of $J^\pi = 8^+$, 11^-, 17^- levels is also observed for $N = 86$ nuclei as protons are removed.[1] The apparent symmetry in the effect for both proton and neutron systems suggests that the phenomenon is not due to some specific aspect of the proton-neutron (or proton-neutron hole) interaction, but rather should be viewed as a more general property, possibly linked to deformation, affecting orbitals of particular quantum numbers irrespective of whether they be occupied by protons or neutrons.

VII. SUMMARY

A detailed spectroscopic investigation of the neutron deficient radon isotopes ^{204}Rn, ^{206}Rn, and ^{208}Rn has been performed. The nuclei exhibit signs of increasing collectivity with decreasing neutron number both in the level patterns of their low-lying states and in their measured transition rates. While $h_{9/2}{}^4$ configurations still appear to dominate the low-lying level structure, some evidence for an increased contribution from the $f_{7/2}$ orbitals is observed, both in the formation of secondary $J^\pi = 6^+$ and 8^+ states in ^{204}Rn, and in the appearance of $J^\pi = 10^-$ isomers. Despite the increase in $B(M1)$ for ^{204}Rn over the other isotopes, no appreciable collective influence was observed in the decay of the $J = 10$ isomers. Systematic behavior for these $Z = 86$ isotopes was discussed in analogy with similar trends in $N = 86$ isotones.

ACKNOWLEDGMENTS

---

*Present address: Department of Nuclear Physics, Australian National University, Canberra, ACT2600, Australia.

†Present address: Schuster Laboratory, Department of Physics, University of Manchester, Manchester, England M13-9L.

[1]C. Baktash, E. der Mateosian, O. C. Kistner, A. W. Sunyar, D. Horn, and C. J. Lister, Contributed

Abstract, the International Conference on Nuclear Physics, Berkeley, 1980 (Report No. LBL-11118) p. 323, and references therein.

[2]D. Horn, O. Häusser, T. Faestermann, A. B. McDonald, T. K. Alexander, J. R. Beene, and C. J. Herrlander, Phys. Rev. Lett. 39, 389 (1977).

[3]T. K. Lönnroth, thesis, University of Jyväskylä, 1980, Research Report No. 3 (1980).

[4]A. R. Poletti, T. P. Sjoreen, D. B. Fossan, U. Garg, A. Neskakis, and E. K. Warburton, Phys. Rev. C 20, 1768 (1979), and private communication.

[5]T. K. Lönnroth, D. Horn, C. Baktash, C. J. Lister, and G. R. Young (unpublished).

[6]T. Inamura, S. Nagamiva, A. Hashizume, Y. Tendow, and T. Katou, Institute of Physical and Chemical Research, Tokyo, Annual Report, 1970, p. 71.

[7]B. G. Ritchie, thesis, University of South Carolina, 1979

(unpublished), and private communication.

[8]H. Backe, Y. Gono, E. Kankeleit, L. Richter, F. Weik, and R. Willwater, Annual Report, Max Planck Institut, Heidelberg, 1977, p.121.

[9]H. Backe, E. Kankeleit, L. Richter, F. Weik, and R. Willwater, Annual Report, Max Planck Institut, Heidelberg, 1979, p.93.

[10]F. Rösel, H. M. Fries, K. Alder, and H. C. Pauli, At. Data Nucl. Data Tables 21, 291 (1978).

[11]Table of Isotopes, 7th ed., edited by C. M. Lederer and V. S. Shirley (Wiley, New York, 1978), and references therein.

[12]D. Horn, G. R. Young, C. J. Lister, and C. Baktash, Phys. Rev. C 23, 1047 (1981).

[13]D. Horn, O. Hässer, B. Haas, T. K. Alexander, T. Faestermann, H. R. Andrews, and D. Ward, Nucl. Phys. A317, 520 (1979).